Japanese Journal of Applied Physics
Vol. 47, No. 3, 2008, pp. 1833–1837

Diffractive Laser Encoder with a Grating in Littrow Configuration

Ching-Fen KAO*, Sheng-Hua LU[1], Hsin-Mao SHEN[2], and Kuang-Chao FAN[2]

Institute of Electrophysics, Mingdao University, ChanHua, Taiwan 523, Republic of China
[1]*Department of Photonics, Feng Chia University, Taichung, Taiwan 407, Republic of China*
[2]*Department of Mechanical Engineering National Taiwan University, Taipei, Taiwan 106, Republic of China*

(Received August 28, 2007; accepted December 7, 2007; published online March 14, 2008)

In this work, we present a new compact diffractive laser encoder system, which serves as a positional detection apparatus in precision machine applications. The encoder records displacement information in terms of grating period using the Doppler effect. Using the Littrow configuration, the novel encoder provides high alignment tolerances. The design is special such that a change in the gap between the grating and the optical head does not affect the measurements. Therefore, a Michelson interferometer can be added to the system to measure the out-of-plane displacement. This system will be developed as a three-dimensional displacement sensor in the future. Within a measurement distance of 100 μm, even in the laboratory environment, the maximum error is 53 nm and the repeatability is within ±20 nm. [DOI: 10.1143/JJAP.47.1833]

KEYWORDS: diffraction grating, grating interferometer, Doppler effect, Littrow configuration

1. Introduction

Nanopositioning and scanning stages have become increasingly important in nanotechnology applications. To achieve the requirement of nanometer accuracy, laser interferometers are commonly uised to detect the displacement of the stages. Laser interferometers are bulky, expensive and sensitive to atmospheric disturbances.[1)] A substitute that does not have the shortcomings of the laser interferometer is the grating interferometer. The displacement is now in terms of grating period rather than laser wavelength. Faster moving stages generally give rise to larger wobbles or vibrations between the optical head and the grating scale. The mechanical instability degrades the quality of the output signals of the grating interferometer, and thus causes positioning errors.

The effects of mechanical wobbles include the tilts and changes in the gap between the optical head and the grating scale. Wu *et al.* and Chiang *et al.* proposed a rotary or linear encoder that was based on retroreflection[2,3)] to improve the tolerance of the tilts associated with mechanical wobbles. The retroreflection in these encoders supports an interference method with equal path lengths. Therefore, interference fringes of high visibility and contrast are observed when the light source exhibits low coherence. In our previous work,[4)] we introduced a planar encoder, based on the diffraction principle. The design, which uses one grating scale and pairs of retroreflective optics, has the advantage of better tolerance to head-to-scale mechanical wobble. However, the aforementioned studies do not address the change in the head-to-scale gap. Therefore, these systems cannot be developed as a three-dimensional displacement sensor.

In this study, we present a compact laser encoder with high alignment tolerance. The novel auto-collimation design based on the Littrow configuration not only can withstand the tilts associated with mechanical wobble, but also the change in the gap between the grating and optical head does not affect the measurement results. The tolerances of this encoder were analyzed as follows.

*E-mail address: Alicekao@mdu.edu.tw

2. Theory

2.1 *Configurations and operational principles*

The measurement principle of the laser encoder is based on the grating Doppler Effect. In a special case of the grating equation,[5,6)] the light is diffracted back in the incident direction when the grating is in the Littrow configuration. The grating equation is simplified to

$$\theta_q = \theta_\mathrm{i} = \sin^{-1}\frac{\lambda}{2p}, \tag{1}$$

where θ_i is the incident angle, θ_q is the diffractive angle, and p is the period of the grating. The changes in the angular frequencies of beam 1 and beam 2 with respect to the motion of the grating are given by

$$\Delta\omega_1 = \frac{2\pi}{p}\cdot v \tag{2}$$

$$\Delta\omega_2 = -\frac{2\pi}{p}\cdot v, \tag{3}$$

where v denotes the moving velocity of the grating in the x-direction. The Doppler effect is such that the light intensity of the superposition of the two beams can be expressed as

$$\begin{aligned} I &= I_1 + I_2 + 2\sqrt{I_1 I_2}\cos(\Delta\omega_1\cdot t - \Delta\omega_2\cdot t) \\ &= I_1 + I_2 + 2\sqrt{I_1 I_2}\cos\left(4\pi\frac{v}{p}t\right) \\ &= I_1 + I_2 + 2\sqrt{I_1 I_2}\cos\left(4\pi\frac{\Delta x}{p}\right), \end{aligned} \tag{4}$$

where Δx denotes the displacement in the X-direction. Equation (4) indicates that the intensity of the interference signal varies as a cosine function of the grating displacement because of the displacement in the x-direction and the fact that the signal period is given by $p/2$. Nevertheless, the direction of the motion of the grating cannot be determined from eq. (4).

Phase shift signals that include four orthogonal sinusoidal signals (sine and cosine) can be adopted to determine the direction of movement, to eliminate common-mode noise and to increase the resolution by electronic interpolation. Smyth and Moore presented the phase shift method approach in their work on instantaneous phase shifting interferome-

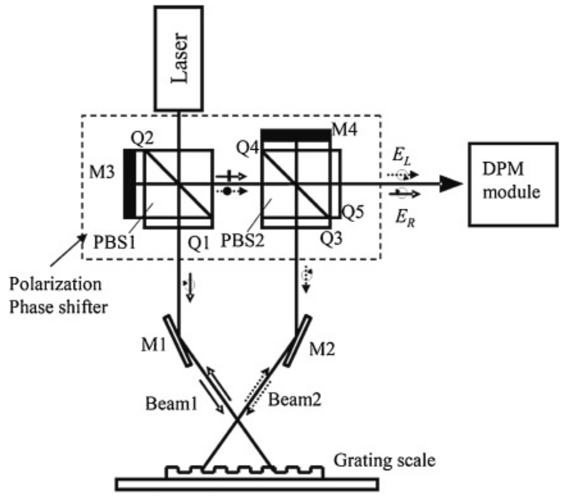

Fig. 1. Basic structure of proposed high-tolerance laser encoder.

try.[7,8] The instantaneous phase shift method is called direct phase measurement (DPM). Figure 1 shows the basic structure of a high-tolerance laser encoder using a polarization phase shifter. This system comprises a laser source, a polarization phase shifter, a grating scale, and a DPM module. The optical path is illustrated as follows.

Beam 1: PBS1 (transmission) → Q1 → M1 → Grating → M1 → Q1 → Q2 → M3 → Q2 → PBS1 → PBS2 (combined with beam 2) → Q5 → DPM

Beam 2: PBS1 (reflection) → PBS2 → Q3 → M2 → Q3 → PBS2 → Q4 → M4 → PBS2 (combined with beam 1) → Q5 → DPM

The polarized beam splitter PBS1 divides the laser beam into two arms with orthogonal polarization (beam 1 with p-polarization and beam 2 with s-polarization). Beam 1, incident on a quarter waveplate, emerges as a right-hand circularly polarized (RHCP) beam. The RHCP beam is reflected by mirror M1 and is incident on the grating scale. The incident angle equals the first-order Littrow diffraction angle. The diffractive beam returns to M1 along the original incident path, and is converted into s-polarized by the quarter waveplate Q1. The s-polarized light is reflected by PBS1, passes through the quarter waveplate Q2, and is reflected by mirror M3. The light that is reflected from mirror M3 twice passes the quarter waveplate Q2, which thus acts as a half waveplate, so beam 1 is p-polarized. Similarly, beam 2, diffracted by the grating scale is returned to M2 along the original incident path. Beam 2, reflected by mirror M4 double-passes the quarter waveplate Q4. Finally, PBS2 combines beam 1 and beam 2 with orthogonal polarization. Beam 1, incident on Q5 emerges as an RHCP beam with electric field E_R, and beam 2 is a left-hand circularly polarized beam (LHCP) with electric field E_L. The transverse vibrations of electric fields E_L and E_R in terms of the Jones Vector are given by

$$\begin{aligned} E_L &\propto A\exp\left[i\left(-\frac{\Delta\omega}{2}\right)t\right]\begin{bmatrix}1\\-i\end{bmatrix}, \\ E_R &\propto A\exp\left[i\left(+\frac{\Delta\omega}{2}\right)t\right]\begin{bmatrix}1\\i\end{bmatrix}, \end{aligned} \tag{5}$$

where A represents the amplitude of the electric field. Equations (2) and (3) yield $\Delta\omega$.

$$\Delta\omega = \Delta\omega_1 - \Delta\omega_2 = 4\pi\frac{\nu}{p} \tag{6}$$

The incidence of two beams on the directed phase measurement (DPM) module produced four interference signals with a relative phase shift of 90°.[4] Therefore, the four signal intensities obtained using the photodetectors are given by

$$\begin{aligned} I_{PD1} &= 2A^2[1+\cos(\Delta\omega\cdot t)] \\ I_{PD2} &= 2A^2[1-\cos(\Delta\omega\cdot t)] \\ I_{PD3} &= 2A^2[1+\sin(\Delta\omega\cdot t)] \\ I_{PD4} &= 2A^2[1-\sin(\Delta\omega\cdot t)]. \end{aligned} \tag{7}$$

The four orthogonal sinusoidal signals (sine and cosine) can be used to calculate the direction of movement, to eliminate common-mode noise and increase the resolution by interpolation.

2.2 *Alignment tolerance analysis*

Higher operating speeds of the machines typically correspond to larger mechanical wobbles or vibrations. Wobbles or vibrations between the optical head and the motion stage, where the grating scale is mounted, directly affect the quality of the optical signals, and therefore cause the optoelectronic signals to decay or even to disappear. Figure 2 shows the five degrees of freedom between the grating scale and the optical head.

The three-dimensional grating diffraction module[9] is used when wobbles occur. As revealed in Fig. 2, the three-dimensional grating diffraction module can be described as

$$\begin{aligned} \hat{e}_{xm} &= \left[-\sin\theta\cos\phi + \frac{m\lambda}{d}\right]\hat{\imath}, \\ \hat{e}_{ym} &= \sin\phi\hat{\jmath}, \\ \hat{e}_{zm} &= \sqrt{1-\sin^2\phi - \left(-\sin\theta\cos\phi + \frac{m\lambda}{d}\right)^2}\,\hat{k}, \end{aligned} \tag{8}$$

where $\hat{e}_{xm}$, $\hat{e}_{ym}$, and $\hat{e}_{zm}$ represent the unit vector components of the diffraction ray; ϕ denotes the elevation angle of the incident beam, and θ is the azimuth angle. The effect of mechanical wobbles is analyzed as follows.

2.2.1 *Pitch motion of grating*

The 2-D diffractive equation can also be used when the grating exhibits pitch as shown in Fig. 3. The incident angle

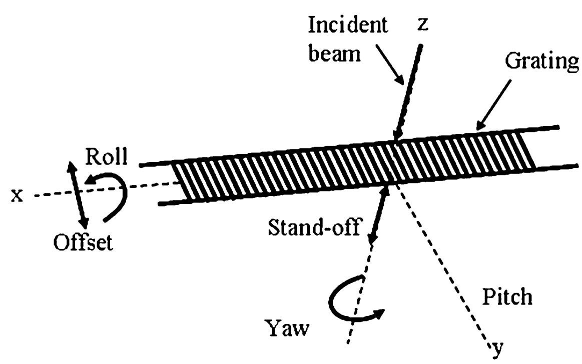

Fig. 2. Five degrees of freedom between grating scale and optical head.

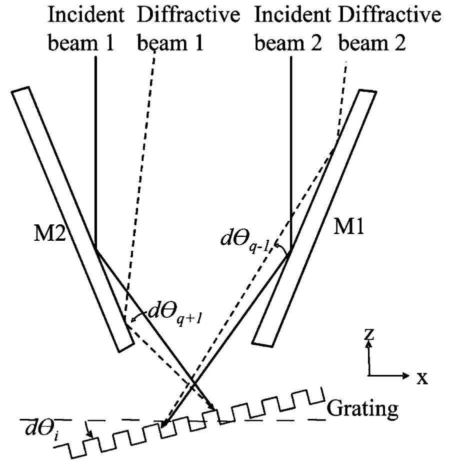

Fig. 3. Change in optical path with pitch of the grating.

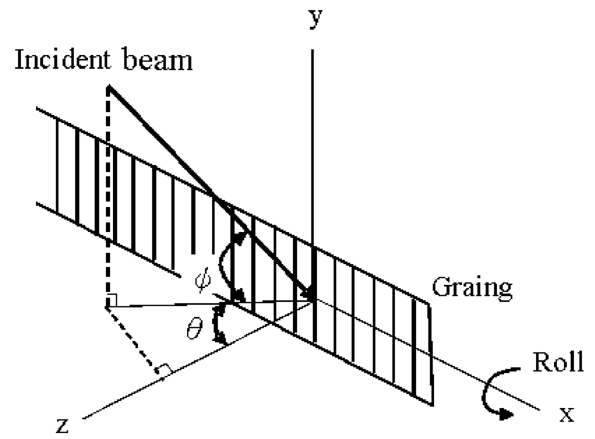

Fig. 4. Sketch of system during roll motion of grating. The fringe of the grating lies along the y-axis. The roll motion of the grating refers to a situation in which the incident light is not perpendicular to the y-axis.

changes by $d\theta_i$ as the pitch angle changes by $d\theta_i$. The change in the diffractive angle is calculated from the grating equation

$$d\theta_q = -\frac{\cos\theta_i}{\cos\theta_q}d\theta_i \tag{9}$$

The incident angles of beam 1 and beam 2 vary in the same direction as pitch motion occurs. According to eq. (9), the changes in the diffraction angles of beam 1 and beam 2 are given by

$$d\theta_{q-1} = d\theta_{q+1} = -\frac{\cos\theta_i}{\cos\theta_q}d\theta_i \tag{10}$$

In the Littrow configuration, $\theta_i = \theta_q$, the changes in the diffraction angles equal to the pitch angle: the two diffractive beams are parallel and combined together by PBS2 with the same position shift on a detector. Consequently, the pitch motion shifts the position of the beams on the detector but does not affect the interference between the two diffractive beams. The tolerance depended only on the size of the detector.

2.2.2 *Roll motion of grating*

The grooves of the grating lie along the y-axis. Roll motion of the grating refers to a situation in which the incident light is not perpendicular to the y-axis (Fig. 4). The three-dimensional grating diffraction module is applied. Figure 5 shows the change in the diffractive angle that is associated with the roll motion of the grating. The diffraction angles of the right beam and left beam are

$$\begin{aligned}\theta'_{q-1} &= \theta_{q-1} + d\theta_{q-1} = \sin^{-1}\left(\sin\theta_i\cos\phi - \frac{\lambda}{d}\right)\\ \theta'_{q+1} &= \theta_{q+1} + d\theta_{q+1} = \sin^{-1}\left(-\sin\theta_i\cos\phi + \frac{\lambda}{d}\right)\end{aligned} \tag{11}$$

Because θ_{q-1} equals $-\theta_{q+1}$, $d\theta_{q-1}$ equals $-d\theta_{q+1}$. The two diffractive beams are distant from each other on the xz plane. If φ is small, then the change in the angle of the diffractive beams $d\theta_{q-1} = -d\theta_{q+1}$ is approximately zero.

However, the two diffracted beams are deviated by the same angle from the y-direction. Therefore, the effect of roll motion in the y direction is to shift the beams on the detector, but not to alter the interference between the two diffractive beams.

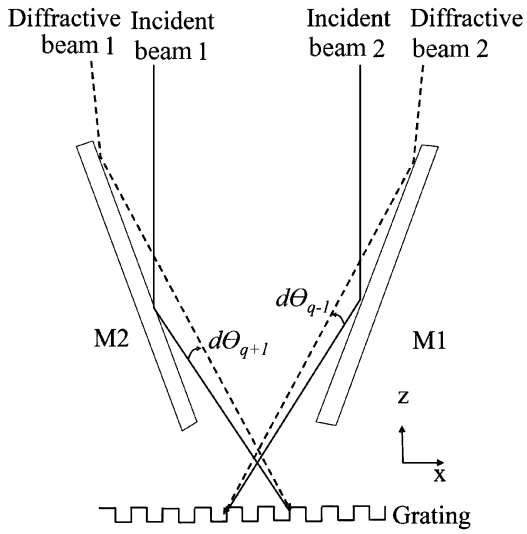

Fig. 5. Change in diffractive angle with roll motion of grating.

2.2.3 *Yaw motion of grating*

The xz plane, which comprises the incident beam and two diffractive beams, is perpendicular to the grating fringes. Therefore, the angle ϕ of yaw of the grating makes the two diffractive beams oblique, and thus removes the two mutually interfering beams from each other. Therefore, the effect of yaw motion is difficult to compensate for this encoder system. In this study, we used LightTools, an optical analysis software for package for analyzing the tolerance of yaw motion. The center distance between two interfering beams was 0.25 mm when the yaw motion was 16 arcmin.

2.2.4 *Gap between grating and optical head*

Figure 6 shows the effect of a change in the gap. According to the Littrow configuration design, the diffractive angle equals the incident angle. Hence, the gap between the grating and the optical head does not affect the interference signal.

As stated above, the proposed encoder can improve the tolerances of the yaw motion of the grating, the roll motion

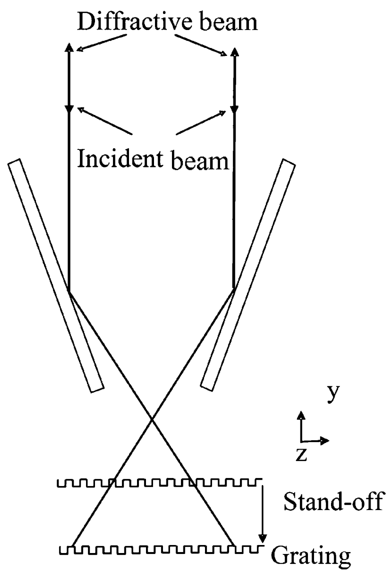

Fig. 6. Effect of change in gap. The gap does not affect the interference signal.

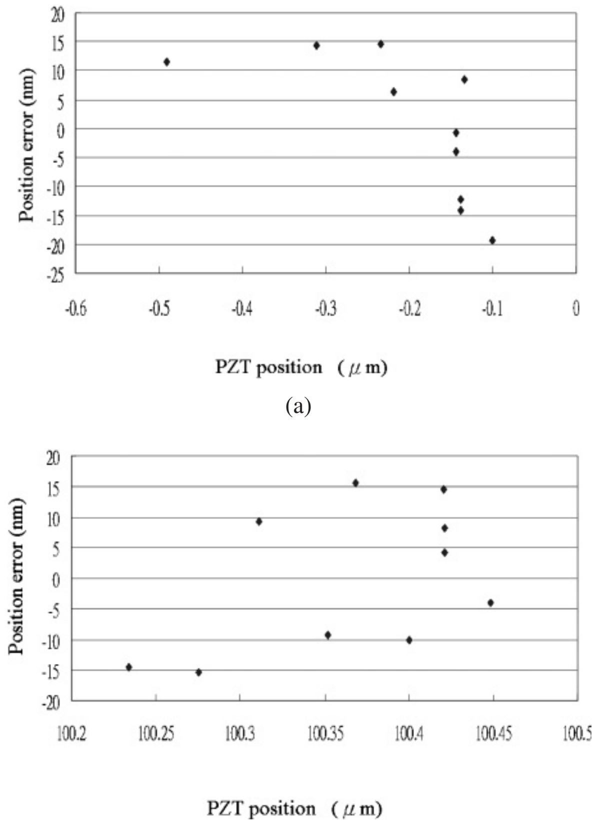

Fig. 7. The stage was programmed to move linearly back and forth 10 times through 100 μm. (a) Repeatability at starting point. (b) Repeatability at terminal point.

of the grating, and the gap between the grating and the optical head.

3. Experiment and Results

The proposed encoder provides an interference scheme with equal path lengths. This equal path configuration yields a fringe contrast of nearly 100%. Therefore, a low-coherence light source, such as a diode laser, can be adopted. In this study, we used a diode laser with a wavelength of 650 nm, guided by a fiber and collimated by a lens, as a light source. The grating pitch was 0.8 μm, the detector size was $4 \times 4\,\text{mm}^2$, the beam size of the splitters was $5 \times 5\,\text{mm}^2$ and the beam diameter of the light source was 1 mm. All the beam splitters and waveplates were in direct contact with each other. The four detectors were pasted on beam splitters. The gap between the optical head and the grating scale was 5 mm. Table I shows the alignment tolerance analyzed using LightTools.[10] The alignment tolerance is defined as follows:

1. The distance between two interference spots must be less than a quarter of the beam diameter.
2. The signal must be greater than 50% of the maximum intensity.

A piezo positioning system of 100 μm scanning range and nanometer resolution was used to measure the accuracy of the encoder. The positioning system included a flexure stage with a high mechanical stiffness and highly accurate guidance, a linearity of 0.1% and a repeatability of ±5 nm provided using an internal capacitance sensor (Cap. Sensor). The period of the sinusoidal signals from the encoder head was 0.4 μm, which is half the scale pitch. The signal period was subdivided using a counter board with an interpolation factor of 400 (Heidenhain IK 220),[11] leading to a readout resolution of approximately 1 nm.

Table I. Alignment tolerance analyzed.

Wobbles of grating	Alignment tolerance	Other work[12]
Pitch (deg)	1.56	1.9
Roll (arcmin)	99	75
Yaw (arcmin)	16	15
Stand-off (mm)	>10	0.5

In this study, we used a laser interferometer, SIOS MI5000, as a reference. The stage was programmed to move linearly back and forth ten times through 100 μm. Figure 7(a) shows the repeatability at the starting points of ten times motion and Fig. 7(b) shows that at the terminal points. The horizontal axis represents the position reading of the encoder. The vertical axis represents the deviation, defined as $x_e - x_r$, where x_e is the readout of encoder and x_r denotes the readout of the interferometer. Figure 8 plots the position errores between encoder and interferometer when the stage moves through 100 μm. The deviations were less than ±28 nm. For the tolerance test, the gap between the optical head and grating scale was changed from 5 to 15 mm in steps of 2 mm. However, the interference signals were not lost when the gap was changed.

4. Conclusions

In this study, we introduce a compact laser encoder based on the grating Doppler effect using a grating in the Littrow configuration. The encoder can improve the tolerances of the tilt motion of the grating by more than 1.5 degrees. Even the gap between the grating and the optical head does not affect the measurement results. Within a measurement distance of 100 μm, even in the laboratory environment, the maximum error is 53 nm and the repeatability is within ±20 nm. The polarization phase shifter not only supplies the phase shift

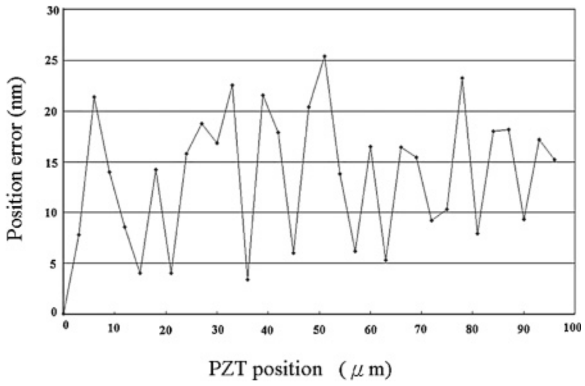

Fig. 8. Position errores between encoder and interferometer when stage moves through 100 μm.

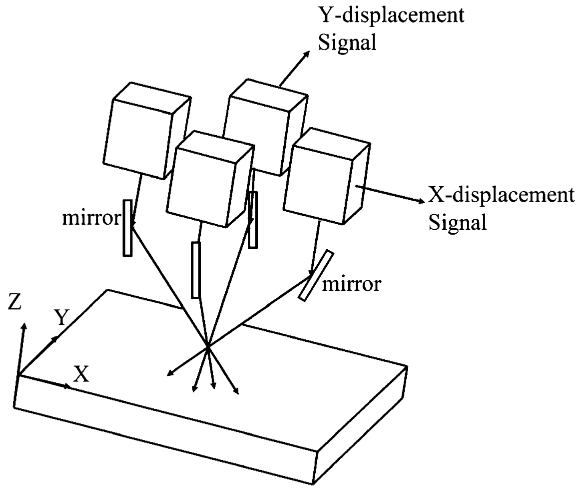

Fig. 9. Schematic of planar encoder.

signal but also reduces the loss of light in the beam splitting process. The design of the interferometer is special such that a change in the gap between the grating and the optical head does not affect the measurements. Therefore, the Michelson interferometer can be added to the system to measure the out-of-plane displacement in the future. A planar encoder can also be developed (Fig. 9) using a planar grating.[4)] The novel grating interferometer can be used to simplify the fabrication of sensors and can be used to produce an easy-to-use three-dimensional displacement sensor, which is likely to be very useful for the semiconductor industry, nanotechnology and materials science.

Acknowledgment

The authors would like to thank the National Science Council of the Republic of China, Taiwan, for financially supporting this research under contract No. NSC 96-2221-E-451-006.

1) M. L. Schattenburg and H. I. Smith: Proc. SPIE **4608** (2002) 116.
2) C.-C. Wu, Y.-C. Chen, C.-K. Lee, C.-T. J. Hsieh, W.-J. Wu, and S.-S. Lu: Proc. SPIE **3779** (1999) 73.
3) W.-W. Chiang and C. K. Lee: U.S. Patent No. 5,442,172 (1995).
4) C. F. Kao, Sh. H. Lu, and M. H. Lu: Rev. Sci. Instrum. **76** (2005) 085110.
5) E. Hecht: *Optics* (Addison-Wesley, Reading, MA, 1998) 4th ed.
6) F. L. Pedrotti and L. S. Pedrotti: *Introduction to Optics* (Prentice-Hall, Englewood Cliffs, NJ, 1996) 2nd ed.
7) R. Smyth and R. Moore: Opt. Eng. **23** (1984) 361.
8) N. R. Sivakumar, W. K. Hui, K. Venkatakrishnan, and B. K. A. Ngoi: Opt. Eng. **42** (2003) 367.
9) R. Petit: *Electromagnetic Theory of Gratings* (Spring-Verlag, Heidelberg, 1990).
10) LightTools User Guide, ORA Manual (ORA, 2000).
11) IK220 PC Counter Card User's Manual (Heidenhain Corp., 2002).
12) C. C. Wu, W. J. Wu, Z. S. Pan, and C. K. Lee: Appl. Opt. **46** (2007) 3169.